Various Implementations of a Statistical Cloud Scheme in COSMO model

Euripides Avgoustoglou

Hellenic National Meteorological Service, El. Venizelou 14, Hellinikon, Athens 16777, Greece

1 Introduction

The starting assumption towards the implementation of cloud cover in numerical weather prediction is that air inside all grid box volume is considered either saturated or unsaturated (Refs. [1], [2],[3]). From the physics standpoint however, this is an approximation to a very complex proccess (Refs. [4]). An obvious shortcoming of this hypothesis is that latent heat is released when condensation process occurs inside the grid box only after all its volume, is at least, saturated which might lead to an incorrect treatment to the initial cloud growth. Also, cloud cover might be affected by entrainmnet through grid box boundaries.

In order to partially account for these processes, in the radiation scheme of COSMO model, an alternative to default sub-grid scheme, based on relative humidity (denoted as SGRH), is proposed to account for the stratiform cloud-cover. In the emerging sub-grid *statistical* scheme (denoted as SGSL), a bivariate Gaussian distribution is invoked for the quasi-conservative properties of *saturation deficit* and *liquid water potential temperature* (Refs. [5], [6]). Within the context SGSL however, the cloud cover due to cloud ice content is treated in a rather naive fashion by simply stating cloud cover equal to 100% if *any* cloud ice is forecasted by the model. The resulting stratiform cloud cover from the implementation of SGSL in COSMO model is given by a two-parameter relation with respect to *cloud cover at saturation* and the *critical value at saturation deficit* (Refs. [7], [8]). The SGSL scheme is currently used in the moist turbulence scheme and the goal is to justify its use also in the radiation scheme within the scope of UTCS (Unified Turbulence Closure Scheme) priority project.

Additionally, the necessity for the effect of cloud-ice into the cloud cover (Refs. [9], [10]) led to a modification of SGSL to a sub-grid statistical liquid-ice scheme (denoted as SGSLI) (Ref. [11]) through the introduction of a mixed phase condensation heat via an *icing factor* defined as the ratio of cloud ice over total cloud water content.

As a part of a systematic investigation under the UTCS project, a comparison of the implementation of SGSL and SGSLI versus SGRH in the radiation scheme of COSMO model is presented over the wider geographical domain of the Balkans for a representative winter case with extended areas of stratiform clouds developed over a relatively weak wind field.

2 Analysis

For the implementation of the statistical cloud scheme the works of Sommeria and Deardorff (Ref. [5]) as well as Mellor (Ref. [6]) were followed. The subgrid low cloud fraction R and mean liquid water content $\overline{q}_l$ are estimated as

$$R = \int_{-\infty}^{\infty}\int_{-\infty}^{\infty} H(q_w - q_s) G dq_w d\theta_l \tag{1}$$

and

$$\overline{q}_l = \int_{-\infty}^{\infty}\int_{-\infty}^{\infty} (q_w - q_s) H(q_w - q_s) G dq_w d\theta_l \tag{2}$$

where q_w and q_s correspond to the total-water and saturation specific humidities respectively, θ_l is the liquid water potential temperature, H stands for the Heaviside function

$$H = \begin{cases} 0, & x < 0 \\ 1, & x > 0 \end{cases} \tag{3}$$

and G is a bivariate normal function

$$G = \frac{1}{2\pi\sigma_{\theta_l}\sigma_{q_w}(1-r^2)^{\frac{1}{2}}} exp\left[\frac{-1}{1-r^2}\left(\frac{\theta_l'^2}{2\sigma_{\theta_l}^2} - r\frac{\theta_l' q_w'}{\sigma_{\theta_l}\sigma_{q_w}} + \frac{q_w'^2}{2\sigma_{q_w}^2}\right)\right] \tag{4}$$

with primed quantities defined as $x' \equiv x - \overline{x}$ and the correlation factor $r = \overline{\theta_l' q_w'}/(\sigma_{\theta_l}\sigma_{q_w})$.

By assuming a linear approximation for q_s around the value $\overline{q}_{sl} = q_s(\overline{\theta}_l, \overline{p})$ and with the help of Clausius-Clapeyron equation the expressions for R and $\overline{q}_l$ become

$$R \approx \frac{1}{2}\left[1 + erf\left(\frac{Q}{\sqrt{2}}\right)\right] \tag{5}$$

$$\overline{q}_l \approx \frac{\sigma}{1+\beta\overline{q}_{sl}}\left[RQ + \frac{exp\left(\frac{-Q^2}{2}\right)}{\sqrt{2\pi}}\right] \tag{6}$$

where

$$Q = \frac{\overline{q}_w - \overline{q}_{sl}}{\sigma}, \qquad \sigma = (\overline{q_w'^2} + \overline{q_{sl}'^2} - 2\overline{q_w' q_{sl}'})^{\frac{1}{2}}, \qquad \beta = 0.622\frac{L^2}{R_d c_p T_l^2} \tag{7}$$

with T_l standing for the liquid water temperature, L is the latent heat for vaporization, R_d is the gas constant for dry air and c_p is the specific heat at constant pressure.

Sommeria and Deardorff (Ref. [5]), further approximated R through the linear part of an empirical curve that they drew for R by using an ensemble of 400 bivariate normal distributions

$$R \approx 0.5(1 + \frac{Q}{1.6}), \qquad 0 \leq R \leq 1 \tag{8}$$

In the statistical cloud scheme implemented in COSMO model, the low cloud cover is parameterized through a similar relation

$$R \approx A(1 + \frac{Q}{B}), \qquad 0 \leq R \leq 1 \tag{9}$$

The parameters A (cloud cover at saturation) and B (critical value of the saturation deficit) are denoted as *clc_diag* and *q_crit* and are tunable in the physical parameterization of COSMO model code. The default values of these parameters used in the present work were chosen to be 0.5 and 4.0 respectively.

Towards the evaluation of the validity of the cloud cover schemes, SGSL and SGSLI were tested in reference to the default SGRH scheme. But in order to further gauge how SGRH is perturbed by the statistical schemes mainly due to cloud-ice, three additional implementations were added and are inscribed as follows,

SGSL_I7 : SGSL is activated in COSMO_V4.11 and cloud cover is set 100% if cloud-ice is more than 10^{-7} Kg/Kg.

SGSL_low : SGSL is activated in the lower troposphere while the default SGRH scheme remains in the upper troposphere.

SGS_L_RH : SGSL is activated for grid points with *no* cloud-ice and SGRH scheme is used for the rest of the grid points.

Although these implementations are rather artificial, they contribute towards a better understanding of the *relative* value of SGSL/SGSLI versus SGRH schemes

3 Case Study

A 48-hour period was considered, starting from 12 UTC of December 24 2007. The boundary conditions came from a three-hour interval GME analysis on forty vertical levels and with horizontal grid of 0.05^0 ($\sim$ 50 Km). The domain under consideration (Fig. 1) covers the wider Balkan having domain of Greece in the center. In all implementations COSMO_V4.11 was utilized except for the test version SGSLI which is based on COSMO_V4.6. On the synoptics standpoint (Fig. 2), from the mean sea level pressure and 500 Hpa geopotential analysis charts, we may see that there was a relatively weak south-western wind field over the region. This feature, combined with the relatively cold air in the lower (850 Hpa) and middle troposphere (500 Hpa), led to extensive cloud cover rich in cloud-ice content as can can be inferred from the relative humidity analysis at 700 HPa.

Regarding radiation budgets (Fig. 3), it was found that there are relative differences especially for the thermal radiation budgets. The thermal radiation budgets at the top of the atmosphere showed that there was more outgoing thermal radiation from the implementation where the relative umidity scheme was invoked (i.e SGRH, SGSL_low, SGS_L_RH implementations). Correspondingly, the thermal radiation budgets at the surface showed that there was less outgoing thermal radiation from the default implementation of the relative humidity SGRH scheme.

Looking at the average cloud cover (Fig. 4), less high clouds were produced when the relative humidity scheme was invoked (i.e SGRH, SGSL_low, SGS_L_RH implementations). More medium and low clouds are produced from the default SGRH scheme while the SGSLI produced the least medium and low clouds

In the upper six-figure panel of Figs. 5 and 6 the total cloud cover of SGRH (upper left), SGSL (upper middle), SGSLI (lower left), SGSL_low (lower middle) and SGS_L_RH (lower right) were presented in reference to an infrared satellite picture. The encircled areas show that the relative differences favored slightly the statistical scheme in any of its implementations against the default SGRH. The other three panels show the cloud cover components for all implementations. In the first panel, the SGSL_I7 scheme was missed but it generally gave the same cloud cover as SGSL scheme.

An impact of cloud cover on 2m temperature is presented for Aghialos meteorological station which is positioned at the Central-East coast of mainland Greece (Fig. 8) against observations and in reference to its cloud cover (Fig. 7) Again the temperature profile is improved when the statistical scheme is used.

4 Summary and Outlook

The cloud cover was found sensitive to the statistical cloud scheme and looks consistent with the default SGRH scheme to the extent of a perturbation. Cloud cover patterns were similar for all implementations but less high clouds were produced when SGRH scheme was invoked. Also,more medium and low clouds were produced by the SGRH default scheme. However the statistical scheme is tunable and this can be modified (current research). Significant differences were found over thermal radiation budgets. Especially those at the top of the atmosphere can be further compared with satellite data. Within the framework provided by this test case as well as several others (Ref. [12]), the subgrid cloud cover scheme looks like a flexible alternative to the default scheme of COSMO model.

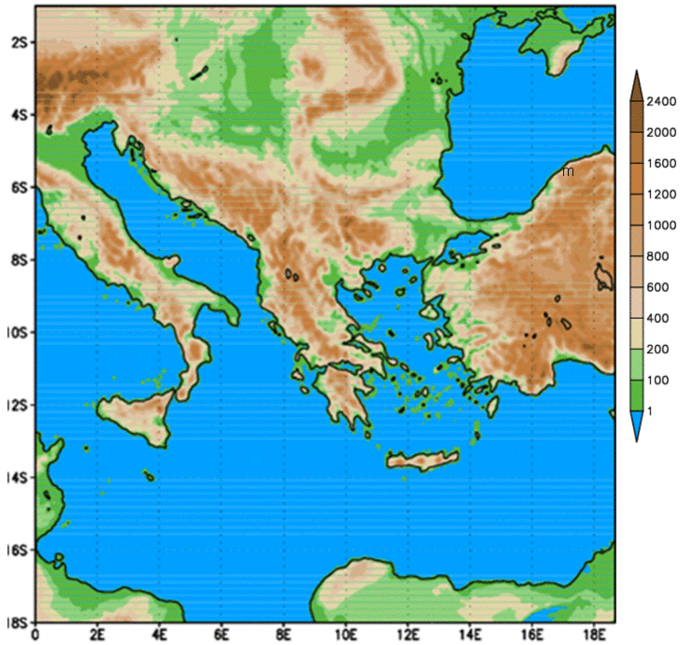

Figure 1: Domain of COSMO runs.

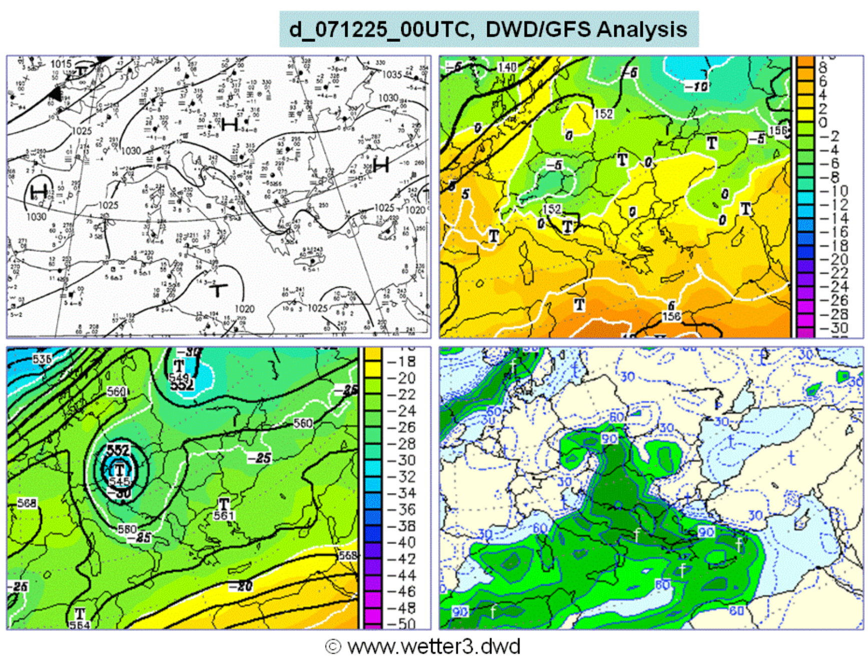

Figure 2: Surface (upper left) 850 Hpa (upper right), 500 Hpa (lower left) and 700 Hpa relative humidity (lower right) analysis at 00 UTC on the 25^{th} of December 2007.

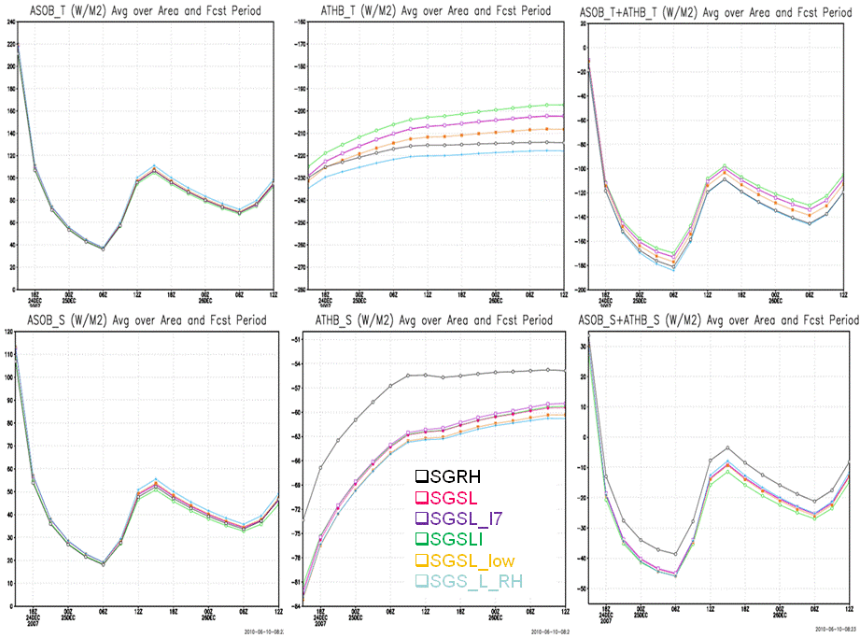

Figure 3: Average radiation balance for a 48-hour period starting from 12 UTC 24-12-2007. The upper left, middle and right figures show the solar, thermal and total radiation budgets at the top of the atmosphere. The lower left, middle and right figures show the solar, thermal and total radiation budgets at the surface.

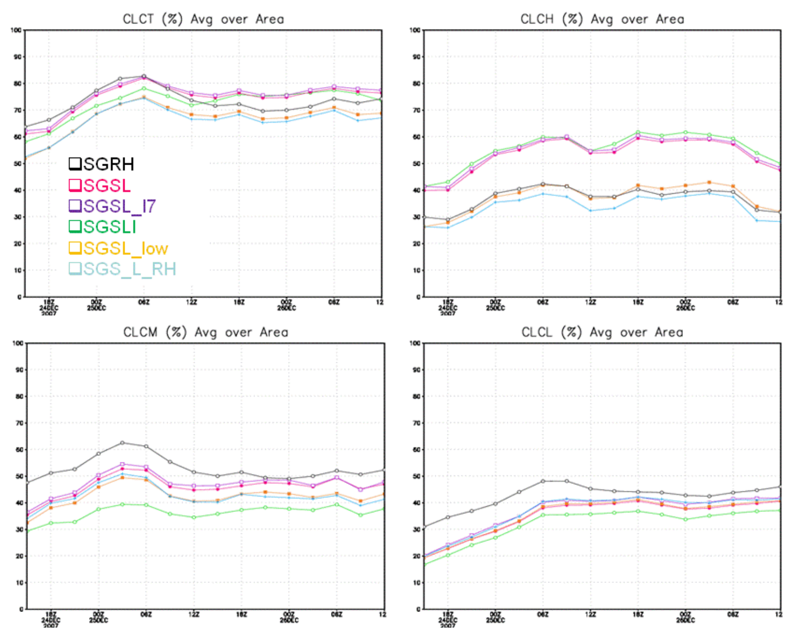

Figure 4: Average cloud cover for the different schemes over the domain and for a 48-hour period starting from 12 UTC 24-12-2007. Total, high, medium and low cloud cover is shown in upper left, right; lower left and right figures respectively

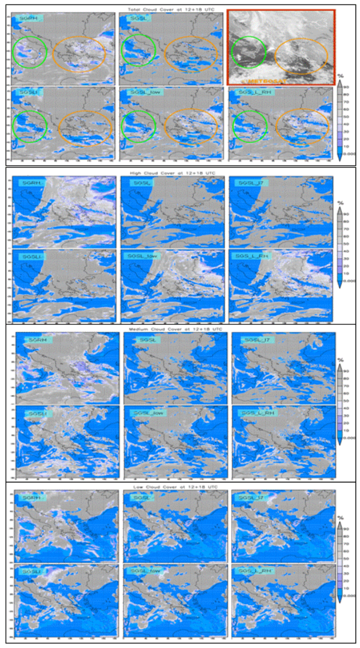

Figure 5: Cloud cover at 12 + 18UTC (i.e. 25-12-2007 ar 06 UTC) for the different cloud schemes. From the top: The first six-figure panel from the top depicts the total, the second the high, the third the medium and the forth the low cloud cover. In every panel the figures are arranged as follows: upper left SGRH, middle SGSL, right SGSL_I7 (replaced by the infrared satelite picture in the total cloud cover panel); lower left SGSLI, middle SGSL_low, right SGS_L_RH.

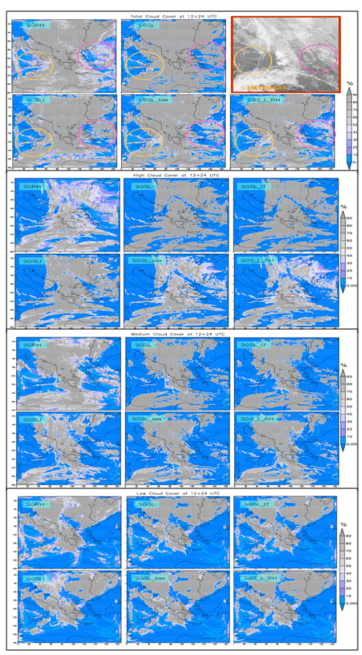

Figure 6: Cloud cover at 12 + 24UTC (i.e. 25-12-2007 ar 12 UTC)for the different cloud schemes. From the top: The first six-figure panel from the top depicts the total, the second the high, the third the medium and the forth the low cloud cover. In every panel the figures are arranged as follows: upper left SGRH, middle SGSL, right SGSL_I7 (replaced by the infrared satelite picture in the total cloud cover panel); lower left SGSLI, middle SGSL_low, right SGS_L_RH.

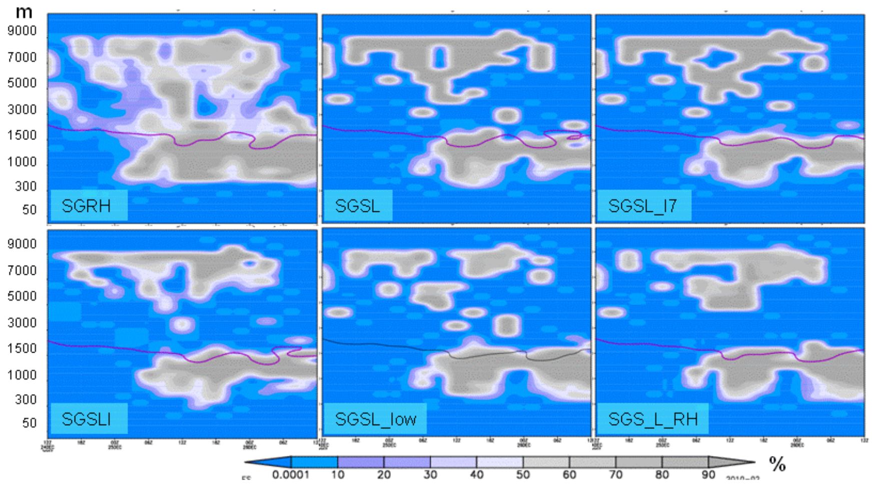

Figure 7: Profiles of cloud cover over Aghialos (Station #16665) for the different Cloud Cover Schemes in 3-hour intervals. The 48-hour Period starts from 12 UTC 24-12-2007. The vertical axis corresponds to model levels and is not linear with height. The purple curve depicts the 0^o C isotherm

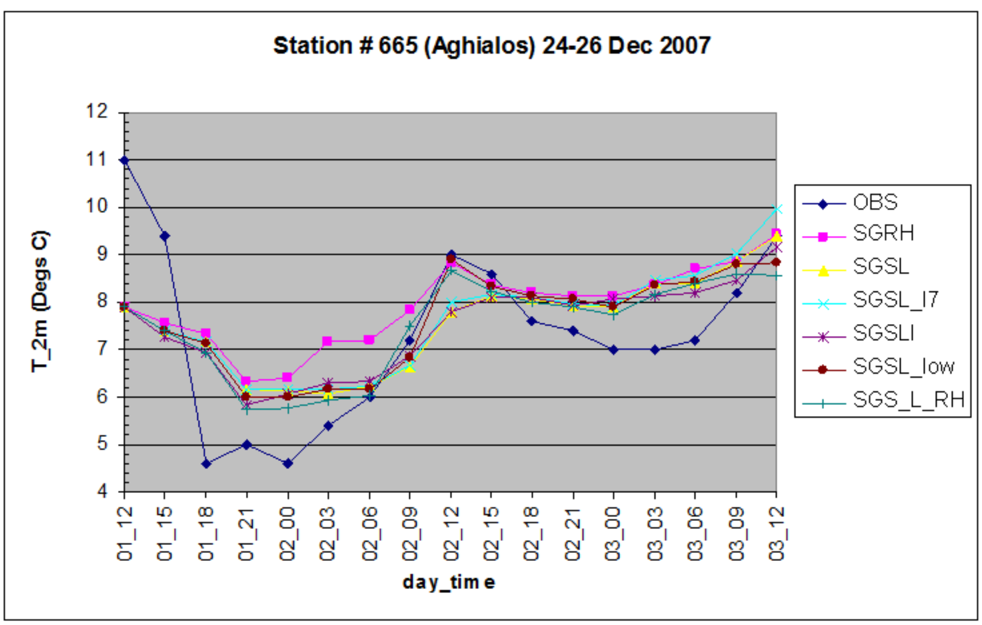

Figure 8: Profiles of 2m Temperatures over Aghialos (Station #16665) for the different Cloud cover Schemes in 3-hour intervals. The 48-hour Period starts from 12 UTC 24-12-2007.

References

[1] R. D. Schlesinger, 1973: A numerical model of deep moist convection: PartI. Comparative experiments for variable ambient moisture and wind shear. *Journal of the Atmospheric Sciences*, **30**, 835-856.

[2] J. T. Steiner, 1973: A three-dimensional model of cumulus cloud development. *Journal of the Atmospheric Sciences*, **30**, 414-435.

[3] G Sommeria, 1976: Three-dimensional simulation of turbulent process in an undisturbed trade wind boundary layer. *Journal of the Atmospheric Sciences*, **33**, 216-241.

[4] D.V. Mironov, 2009: Turbulence in the Lower troposphere: Second-order Closure and Mass-Flux Modeling Frameworks. *Lecture Notes in Physics*, **756**, 161-221.

[5] G. Sommeria and J. W. Deardorff, 1977: Subgrid-Scale Condensation in Models of Non-precipitating Clouds. *Journal of the Atmospheric Sciences*, **34**, 344-355.

[6] G. L. Mellor, 1977: The Gaussian Cloud Model Relations. *Journal of the Atmospheric Sciences*, **34**, 356-358.

[7] M. Raschendorfer, 2005: A new TKE-based Scheme for Vertical Diffusion and Surface-layer Transfer. *DWD Internal Report*.

[8] E. Avgoustoglou, T. Tzeferi, and I. Papageorgiou, 2006: Implementation of the Statistical Cloud Scheme Option; Preliminary Tests. *COSMO Newsletter* **6**, 88-93.

[9] J. W. Deardorff, 1976: Usefulness of Liquid-Water Potential Temperature in a Shallow-Cloud Model. *Journal of Applied Meteorology*, **15**, 98-102.

[10] S. A. Smith and Del A. D. Del Genio, 2002: A simple conceptual conceptual model of cirrus horizontal inhomogeneity and cloud fraction. *Quarterly Journal of the Royal Meteorological Society*, **128**, 149-171.

[11] M. Raschendorfer, 2008: Mixed water/ice phase in the SGS condensation scheme and the moist turbulence scheme. *Presentation*, 10^{th} COSMO General Meeting, Cracow, Poland.

[12] E. Avgoustoglou, 2010: Sensitivity Evaluation of Various Implementations of the SGS Cloud Scheme over Greece. *Presentation*, 12^{th} COSMO General Meeting, Moscow, Russia.